



## CFD Study on Fluidized Bed Pyrolyzers

Ka Leung Lam, Tesfaldet Gebreegziabher, Adetoyese O. Oyedun,  
Ho Kei M. Lee, Chi Wai Hui

Department of Chemical and Biomolecular Engineering, The Hong Kong University of Science and Technology,  
Clear Water Bay, Kowloon, Hong Kong  
[kehui@ust.hk](mailto:kehui@ust.hk)

Fluidized bed pyrolyzers are commonly used for biomass fast pyrolysis to maximize the pyrolysis oil yield. A CFD study was performed on homogeneous secondary pyrolysis reactions that cause a reduction of liquid fraction yield and to propose certain design and operation considerations to reduce the extent of secondary reactions. Two models are utilized for the study. A particle pyrolysis model uses a kinetic model from literature to describe the pyrolysis progress of wood particle. The second model involves the use of commercial CFD code ANSYS FLUENT to model a fluidized bed pyrolysis scenario and secondary reactions based on the modelled pyrolysis progress from the first model. The effects and inter-relationship between feedstock size, fluidized gas temperature, vapour residence time and liquid fraction yield are discussed. It is found that the fluidized gas temperature is a more critical factor than vapour residence time in causing secondary reactions, while feedstock size only has a little effect. In addition, the downward flow of the pyrolysis volatiles observed along the reactor wall has to be considered in the design of the feeding and fluidized bed system.

### 1. Introduction

Pyrolysis is the thermal decomposition of organic materials at elevated temperatures in the absence of oxygen yielding carbonaceous residues, liquid hydrocarbons and combustible gases. Depending on the processing conditions, the yield distribution among the three categories of product can vary a lot. It is found that under a high heating rate pyrolysis condition with a short vapour residence time, the pyrolysis liquid becomes the major product fraction. Fluidized bed reactor is usually employed for this type of pyrolysis, namely fast pyrolysis. This type of pyrolysis has a heating rate in the magnitude of over hundreds degrees per second and therefore, pyrolysis can be completed in a few seconds. The product gas is then quickly removed from the reactor and quenched for condensing the pyrolysis liquid. It is generally agreed that in order to maximize the production of pyrolysis oil, the extent of secondary reactions and the formation of char have to be reduced.

Secondary reactions refer to the further reactions of pyrolysis tar produced from primary pyrolysis reactions. These reactions include condensation, re-polymerization and cracking (Curtis and Miller, 1988). There are two types of secondary reactions. One involves the heterogeneous reaction between the primary tar and the char constituent forming secondary tar, non-condensable fraction and secondary char (Koufopoulos et al., 1991, Antal Jr and Varhegyi, 1995, Sadhukhan et al., 2009). Another type of secondary reactions is the cracking of the primary tar at the high temperature gas phase region forming smaller gas fraction and tar fraction. This homogenous secondary decomposition reactions is suggested to become more prominent at higher temperature (Curtis and Miller, 1988).

Please cite this article as: Lam K.-L., Gebreegziabher T., Oyedun A. O., Lee H. K. M. and Hui C.-W., (2012), CFD study on fluidized bed pyrolyzers, Chemical Engineering Transactions, 29, 661-666

## 2. Problem statement

Fluidized bed pyrolyzer is the subject of study. This work focuses specifically on homogeneous secondary pyrolysis reactions that lower liquid fraction yield. The effects and inter-relationship between feedstock size, fluidized gas temperature, vapour residence time and liquid fraction yield are studied. Some design and operation approaches to reduce the extent of secondary reactions are then proposed.

## 3. Methodology

### 3.1 Overview

This study utilizes two models, a particle pyrolysis model and a reactor model, to describe the pyrolysis of wood particles in a bubbling fluidized bed pyrolyzer. The particle pyrolysis model was developed on MATLAB® platform to simulate the pyrolysis progress of multiple wood particles within a fluidized bed. The reactor model involves the use of commercial CFD code ANSYS FLUENT to model a fluidized bed pyrolysis scenario based on the modelled pyrolysis progress from the particle pyrolysis model. As shown in Figure 1, a simplified wood pyrolysis mechanism (Papadikis et al., 2009, Kaushal and Abedi, 2010) is used in this work. During the primary pyrolysis phase, three fractions of products, pyrolysis gas, oil and char are produced. The pyrolysis oil further undergoes a homogeneous secondary reaction to break down into pyrolysis gas.

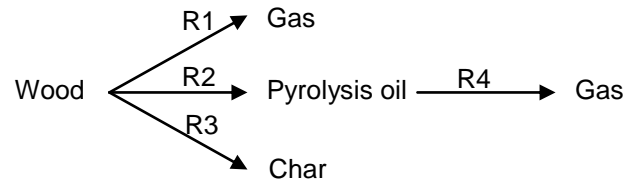


Figure 1: Mechanism of wood pyrolysis

### 3.2 Particle pyrolysis model

The equations listed below describe transiently the pyrolysis progress of a spherical wood particle. The detail description of similar models can be found in some previous works (Cheung et al., 2011, Lam et al., 2011). Eq. 1-6 cover the kinetic mechanism of wood pyrolysis defined in Fig. 1. Eq. 4 is used by the CFD reactor model to account for the homogenous secondary reaction. Eq. 7-11 describes the heat transfer and physical changes of the particle during pyrolysis.

$$\frac{d\alpha_1}{dt} = k_1\alpha_w \quad (1)$$

$$\frac{d\alpha_2}{dt} = k_2\alpha_w - k_4\alpha_2 \quad (2)$$

$$\frac{d\alpha_3}{dt} = k_3\alpha_w \quad (3)$$

$$\frac{d\alpha_4}{dt} = k_4\alpha_2 \quad (4)$$

$$\frac{d\alpha_w}{dt} = -(k_1 + k_2 + k_3)\alpha_w \quad (5)$$

$$k_i = A_i \exp\left(-\frac{E_i}{RT}\right) \quad (6)$$

$$\frac{\partial T}{\partial t} = \frac{\lambda}{\rho_p C_p} \frac{\partial^2 T}{\partial r^2} + \frac{2}{r} \frac{\lambda}{\rho_p C_p} \frac{\partial T}{\partial r} - \frac{H_p}{C_p} \frac{\partial \alpha_w}{\partial t} \quad (7)$$

$$C_p = \frac{\alpha_w}{\alpha_w + \alpha_c} C_{p,w} + \frac{\alpha_c}{\alpha_w + \alpha_c} C_{p,c} \quad (8)$$

$$\lambda = \frac{\alpha_w}{\alpha_w + \alpha_c} \lambda_w + \frac{\alpha_c}{\alpha_w + \alpha_c} \lambda_c \quad (9)$$

$$\text{B.C.s: } -\lambda \frac{\partial T}{\partial r} = h(T_s - T_b) \quad \left. \frac{\partial T}{\partial r} \right|_{r=0} = 0 \quad (10)$$

$$\frac{dV}{dt} = -V_0 \frac{d(\alpha_w + \alpha_3)}{dt} (1 - \delta) \quad (11)$$

### 3.3 Reactor model

A bubbling fluidized bed reactor with a uniform gas inlet at the bottom and a side outlet near the top is defined with the dimension stated in table 1. ANSYS ICEM CFD was used to construct the geometry and the mesh of a cross-section of this fluidized bed reactor. The unstructured quad mesh was then introduced to ANSYS FLUENT 12.0 for developing a model to simulate on the pyrolysis volatiles movement and the homogeneous secondary reaction. Built-in Eulerian multiphase model, laminar flow model, laminar finite-rate model and discrete phase model were utilized. The simulation with the particle pyrolysis model yields the volatile generation profile, including both non-condensable gas and pyrolysis oil. This profile was then transferred to the CFD model for further simulation. To transfer the profiles, an injection zone was defined within the fluidized bed zone. Following the profiles, at a given time, a particular amount of discrete volatiles particles are injected and vaporized simultaneously into the gas phase. Table 1 and table 2 tabulate the key parameters used in both models. Several key assumptions were made in the models:

- 1) Inlet fluidized gas is inert.
- 2) The temperature of the fluidized bed remains steady.
- 3) Pyrolyzing wood particles are fluidized within the defined region during the course of pyrolysis.
- 4) Secondary heterogeneous reactions between primary pyrolysis oil and char are limited.

Table 1: Summary of key model parameters

Parameter (unit)	Value	Reference
Initial density of wood particle, $\rho_p$ (kg/m <sup>3</sup> )	650	(Koufopoulos et al., 1991)
Specific heat capacity of heating gas (J/kg-K)	2400	(Yang et al., 1995)
Thermal conductivity of wood, $\lambda_w$ (W/m-K)	2380	(Ahuja et al., 1996)
Thermal conductivity of char, $\lambda_c$ (W/m-K)	1600	(Ahuja et al., 1996)
Specific heat capacity of wood, $C_{p,w}$ (J/kg-K)	0.158	(Ahuja et al., 1996)
Specific heat capacity of char, $C_{p,c}$ (J/kg-K)	0.107	(Ahuja et al., 1996)
Convective heat transfer coefficient, $h$ (W/m <sup>2</sup> -K)	300	(Papadikis et al., 2010)
Sand density	2500	(Papadikis et al., 2010)
Heat of pyrolysis, $H_p$ (kJ/kg)	-255	(Papadikis et al., 2010)
Sand diameter (mm)	0.5	-
Shrinking factor for wood pyrolysis, $\delta$	0.835	-
Packing limit	0.6	-
Reactor diameter (m)	1.5	-
Reactor height (m)	5	-
Superficial gas velocity (m/s)	1	-
Initial bed height (m)	2	-
Volatiles injection region from reactor inlet (m)	1.5 – 2.5	-

Table 2: Summary of kinetic parameters

Reaction	Pre-exponential factor (s <sup>-1</sup> )	Activation energy (kJ/mol)	Reference
R1	1.43 x 10 <sup>4</sup>	88	(Kaushal and Abedi, 2010)
R2	4.12 x 10 <sup>6</sup>	112	(Kaushal and Abedi, 2010)
R3	7.37 x 10 <sup>5</sup>	106	(Kaushal and Abedi, 2010)
R4	2.6 x 10 <sup>6</sup>	108	(Papadikis et al., 2009)

## 4. Results and discussions

### 4.1 Simulation results of particle pyrolysis model

In the base case, a wood particle of 1mm in diameter is pyrolyzed in a fluidized bed reactor with a heating gas temperature of 550°C, which is a vapour phase temperature proposed by Van de Velden et al. (2010) for limiting secondary reactions. Under such pyrolysis condition, the three fractions of product form with the distribution shown in Fig. 2 and the oil generate rate profile is given in Fig 3.

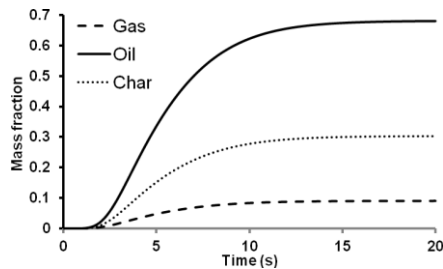


Figure 2: Primary products yield distribution

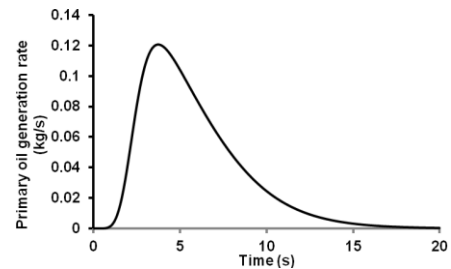


Figure 3: Primary oil generation rate profile

### 4.2 Simulation results of reactor model

The volatiles generation profiles obtained from the particle pyrolysis model was then transferred to the CFD reactor model for further simulation. It is found that under the specified processing condition with the described reactor configuration, the extent of secondary reaction is severe with a loss of primary pyrolysis oil to be around 59.8 %. Figures 4 and 5 show the contours of the studied product species.

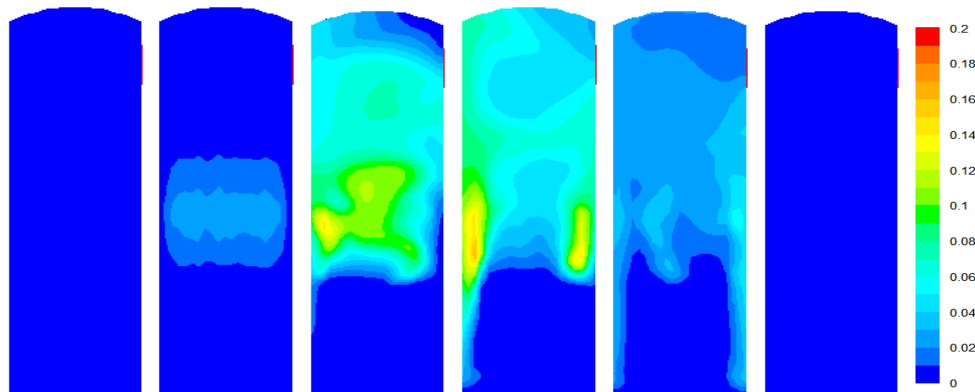


Figure 4: Contours of primary pyrolysis oil concentration at different processing time

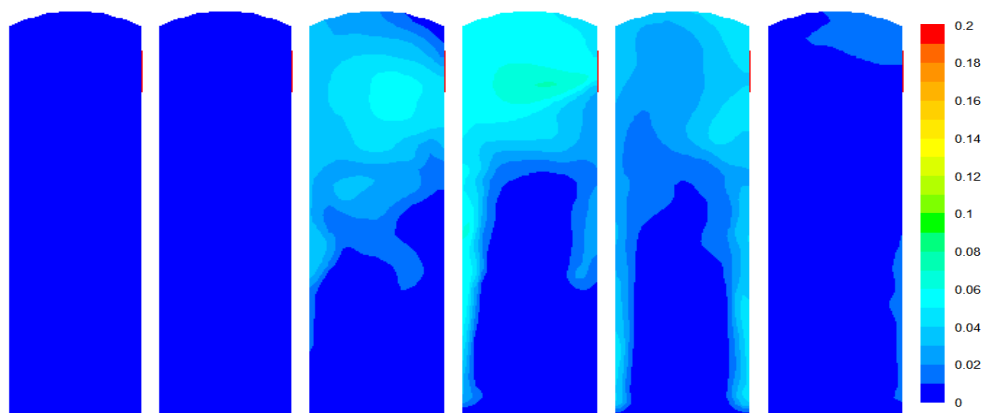


Figure 5: Contours of secondary pyrolysis gas concentration at different processing time

### 4.3 Effect of fluidized gas temperature

The simulation in the previous section was used as the base case for comparison. The temperature of inlet gas was varied to study on its impacts and the results are presented in Table 3. Vapour residence time is defined as the time difference between the maximum primary pyrolysis oil generation time within the bed and the maximum primary oil outflow at the reactor outlet. A higher temperature greatly reduces the pyrolysis time, but promotes secondary reaction.

Table 3: Pyrolysis time, residence time and extent of secondary reactions for different gas temperature

Gas temperature (°C)	Pyrolysis time (s)	Vapour residence time (s)	Extent of secondary reactions (%)
500	34.6	2.9	29.0
550 (base)	17.6	2.5	59.8
600	10.2	1.7	82.4
650	6.6	1.1	95.0

### 4.4 Effect of feedstock size

Different sizes of the feedstock particle were simulated and the results are shown in Table 4. It is found that the size of feedstock only influences the completion time, but has a little effect on the extent of secondary reactions. When the feedstock size reduces, the reactor temperature becomes the limiting factor for pyrolysis rather than the size itself. The consideration of feedstock size is therefore more on an issue of fluidized bed operation and pyrolysis time rather than product yield distribution.

Table 4: Pyrolysis time, residence time and extent of secondary reactions for different feed diameter

Feed diameter (mm)	Pyrolysis time (s)	Vapour residence time (s)	Extent of secondary reactions (%)
0.3	14.3	1.8	57.5
0.5	15.2	2.7	57.3
1 (base)	17.6	2.5	59.8
2	23.2	0.6	56.2

### 4.5 Effect of gas velocity

The gas velocity was not set above that of the base case to prevent any throughflow of fluidizing sand. Under the assumption that the particles are pyrolyzing in the defined region, the gas velocity obviously governs the vapour residence time, which in turn, dictates the extent of secondary reaction. At a lower gas velocity, although it has a much longer vapour residence, the gas phase temperature is lower when volatiles are given out by the particles. This reduces the extent of secondary reaction.

Table 5: Pyrolysis time, residence time and extent of secondary reactions for different inlet gas velocity

Gas velocity (m/s)	Vapour residence time (s)	Extent of secondary reactions (%)
0.4	8.4	49.6
0.5	4.1	66.3
0.8	2.9	66.1
1 (base)	2.5	59.8

### 4.6 Minimization of secondary reactions

While the model is a simplified one, it gives a general picture of the effects and the inter-relationship of different processing parameters. The inlet gas temperature, essentially the pyrolysis temperature, plays the key role in determining the extent of secondary reaction and is a more critical factor than the vapour residence time. While designing and operating a fluidized bed pyrolyzer, the reduction of feedstock size has to be first considered to ensure the feedstock size is not the limiting factor. Afterwards, the two key factors, operating temperature and vapour residence time, are in place as variables to be optimized. In addition, in designing the fluidizing system and the feeding system, one has to consider the flow of generated volatiles in such a way to avoid the downward flow of the these volatiles along the reactor surface, as observed in Figure 4.

## 5. Conclusions

A CFD study was performed on homogenous secondary pyrolysis reactions in a fluidized bed scenario. It is found that the fluidized gas temperature is a more critical factor than vapour residence time in causing secondary reactions, while feedstock size only has a little impact. In addition, the downward flow of the pyrolysis volatiles observed along the reactor wall has to be considered in the design of the feeding and fluidized bed.

## Nomenclature

$k$	Reaction rate constant ( $s^{-1}$ )	<i>Subscripts</i>	
$A$	Pre-exponential factor ( $s^{-1}$ )	$w$	Wood
$E$	Activation energy (J/mol)	$c$	Char
$R$	Universal gas constant (J/mol-K)	$i$	Species/ reaction index
$t$	Time (s)	$s$	Particle surface
$T$	Temperature (K)	$b$	Bulk environment
$r$	Radius of a discrete layer (m)		
$h$	Convective heat transfer coefficient ( $W/m^2-K$ )	<i>Greek Letters</i>	
$H_p$	Heat of pyrolysis (kJ/kg)	$\alpha$	Mass fraction of a species
$C_p$	Specific heat capacity (J/kg-K)	$\rho$	Density ( $kg/m^3$ )
$V$	Particle volume ( $m^3$ )	$\lambda$	Thermal conductivity ( $W/m-K$ )
$V_0$	Initial particle volume ( $m^3$ )	$\delta$	Shrinking factor

## Acknowledgement

The authors gratefully acknowledge the Hong Kong RGC research grant (No. 613808, 614307).

## References

- Ahuja P., Kumar S., Singh P. C., 1996, A model for primary and heterogeneous secondary reactions of wood pyrolysis, *Chem. Eng. Technol.* 19, 272-282.
- Antal Jr M. J., Varhegyi G., 1995, Cellulose pyrolysis kinetics: The current state of knowledge, *Ind. Eng. Chem. Rev.* 34, 703-717.
- Cheung K. Y., Lee K. L., Lam K. L., Lee C. W., Hui C. W., 2011, Integrated kinetics and heat flow modelling to optimise waste tyre pyrolysis at different heating rates, *Fuel Process Technol.* 92, 856-863.
- Curtis L. J., Miller D. J., 1988, Transport model with radiative heat transfer for rapid cellulose pyrolysis, *Ind. Eng. Chem. Res.* 27, 1775-1783.
- Kaushal P., Abedi J., 2010, A simplified model for biomass pyrolysis in a fluidized bed reactor, *J. Ind. Eng. Chem.* 16, 748-755.
- Koufopoulos C. A., Papayannakos N., Maschio G., Lucchesi A., 1991, Modelling of the pyrolysis of biomass particles. Studies on kinetics, thermal and heat transfer effects, *Can. J. Chem. Eng.* 69, 907-915.
- Lam K. L., Oyedun A. O., Cheung K. Y., Lee K. L., Hui C. W., 2011, Modelling pyrolysis with dynamic heating, *Chem. Eng. Sci.* 66, 6505-6514.
- Papadakis K., Gu S., Bridgwater A. V., 2010, Computational modelling of the impact of particle size to the heat transfer coefficient between biomass particles and a fluidised bed, *Fuel. Process. Technol.* 91, 68-79.
- Papadakis K., Gu S., Bridgwater A. V., Gerhauser H., 2009, Application of CFD to model fast pyrolysis of biomass, *Fuel Process Technol.* 90, 504-512.
- Sadhukhan A. K., Gupta P., Saha R. K., 2009, Modelling of pyrolysis of large wood particles, *Bioresource Technol.* 100, 3134-3139.
- Van De Velden M., Baeyens J., Brems A., Janssens B., Dewil R., 2010, Fundamentals, kinetics and endothermicity of the biomass pyrolysis reaction, *Renew. Energ.* 35, 232-242.
- Yang J., Tanguy P. A., Roy C., 1995, Heat transfer, mass transfer and kinetics study of the vacuum pyrolysis of a large used tire particle, *Chem. Eng. Sci.* 50, 1909-1922.